Macroscopic modeling of social crowds

Mathematical Models and Methods in Applied Sciences

Macroscopic modeling of social crowds

Livio Gibelli[(1)], Damian Knopoff[(2)], Jie Liao[(3)], and Wenbin Yan[(4)]

[(1)] *School of Engineering*
Institute for Multiscale Thermofluids
The University of Edinburgh, Edinburgh, United Kingdom.
livio.gibelli@ed.ac.uk

[(2)] *Faculty of Engineering, University of Deusto, Avda. Universidades, 24, 48007 Bilbao, Spain and Centro de Investigaciones y Estudios de Matemática, CONICET, Medina Allende s/n, 5000 Córdoba, Argentina.*
d.knopoff@deusto.es

[(3)] *School of Mathematics, Shanghai University of Finance and Economics, Shanghai 200433, China.*
liaojie@mail.shufe.edu.cn

[(4)] *École Polytechnique*
91120 Palaiseau France
wenbin.yan@polytechnique.edu

Received (Day Month Year)
Revised (Day Month Year)
Communicated by (xxxxxxxxxx)

Social behavior in crowds, such as herding or increased interpersonal spacing, is driven by the psychological states of pedestrians. Current macroscopic crowd models assume that these are static, limiting the ability of models to capture the complex interplay between evolving psychology and collective crowd dynamics that defines a "social crowd". This paper introduces a novel approach by explicitly incorporating an "activity" variable into the modeling framework, which represents the evolving psychological states of pedestrians and is linked to crowd dynamics. To demonstrate the role of activity, we model pedestrian egress when this variable captures stress and awareness of contagion. In addition, to highlight the importance of dynamic changes in activity, we examine a scenario in which an unexpected incident necessitates alternative exits. These case studies demonstrate that activity plays a pivotal role in shaping crowd behavior. The proposed modeling approach thus opens avenues for more realistic macroscopic crowd descriptions with practical implications for crowd management.

Keywords: Crowd dynamics, macroscopic model, social dynamics, stress, contagion awareness.

AMS Subject Classification: 82D99, 91D10

1. Introduction

In recent years, a growing number of studies in crowd dynamics have focused on incorporating the social behaviors of pedestrians into modeling. Examples of relevant social behaviors range from herding during crowd evacuations to increased physical distancing during a pandemic. Social behaviors are rooted in the psychological states of pedestrians and shape the collective dynamics of a crowd. In turn, pedestrians' psychological states evolve in response to changing crowd conditions, modifying social behaviors. This complex interplay between psychological states and crowd dynamics defines the concept of the "social crowd".

Over the years, models describing social crowds have been developed at different levels of granularity, from microscopic (individual-based) to mesoscopic (kinetic) to macroscopic (hydrodynamic) (see [7] for a recent review of different scales of crowd modeling). The first seminal contributions were made at the microscopic level, showing that the incorporation of a parameter describing pedestrian stress allows the modeling of several real-world crowd phenomena, such as herding behavior and the faster-is-lower effect [16,17,18]. Subsequent efforts have moved to the mesoscale using the versatile framework of active particle kinetic theory [3]. This approach retains the ability to capture the complex nature of crowds, while alleviating the computational burden associated with microscopic models that require tracking the individual state of each pedestrian [23]. While microscopic and mesoscopic models offer detailed insights, the macroscopic level of description provides an efficient and scalable framework for simulating large crowds in real-world scenarios. Recent notable contributions include a game-theoretic macroscopic model of crowd dynamics for analyzing a variety of scenarios ranging from marathons to drafting in cycling [2], and a model specifically designed for predicting pedestrian movement and correcting congestion [14]. Despite these advances, the macroscopic modeling of social crowds remains largely underexplored with only a few studies including social dynamics [12,21].

A common assumption in all of the above work is that pedestrians' psychological states remain static over time, independent of dynamic crowd conditions, which limits the realism of social crowd modeling. Further advances have been made at the mesoscale to describe panicking crowds. In [8,24] and [5], models have been developed that allows pedestrian stress to evolve in response to changing crowd densities. Related studies have explored how the ability to learn progressively modifies interaction rules and contributes to the development of self-organizing collective intelligence [10], the role of leaders trained to choose safe paths in evacuation [22], and contagious spread within crowds [1,4,19,20].

This paper presents a model that captures the interplay between mechanical and social behavior in crowds at the macroscopic scale, marking the first macroscopic model of a social crowd. Our proposed approach combines a second-order macroscopic crowd model to describe the "mechanical" behavior of the crowd with a transport equation to capture its "social" behavior. The use of a second-order

model to describe the mechanical behavior of the crowd is an additional novelty of this work that should be highlighted. Unlike first-order models, which consider only density as the primary variable, focus on conservation of mass, and establish a velocity-density relationship, the second-order model is distinguished by the inclusion of the velocity balance equation. Although the computational complexity increases [14], this addition significantly improves its ability to accurately represent pedestrian behavior, especially in dynamic scenarios involving pedestrian acceleration or deceleration. It is also noteworthy that the second-order model developed in this paper builds on previous mesocopic crowd models [5] and follows the unified modeling approach across scales outlined in [6].

The rest of the paper is organized as follows. In Section 2, we present the general mathematical formulation of our macroscopic social crowd model, specializing it to consider two different social behaviors, namely stress and contagion awareness. In Section 3, we give a brief overview of the finite volume method used to solve the model numerically. We then present simulation results for two case studies. First, we simulate a pedestrian evacuation where the activity variable captures stress and contagion awareness to demonstrate how different social behaviors can significantly affect crowd dynamics. Second, we simulate a scenario in which an exit door closes unexpectedly to illustrate the importance of incorporating dynamic changes in activity into the model to produce realistic crowd behavior. Finally, in Section 4, we provide a summary of our findings and outline potential avenues for future research.

2. Mathematical formulation

We study the behavior of a crowd in a domain denoted by Ω. The state of the crowd is described by three primary macroscopic fields: density ρ, velocity $\boldsymbol{\xi}$, and activity u. The first two variables describe the "mechanical" behavior of the crowd, while the third variable is designed to capture its "social" behavior. The mathematical model we employ consists of a second-order macroscopic model governing the mechanical variables, coupled with a scalar transport equation for the social variable,

$$\begin{cases} \dfrac{\partial \rho}{\partial t} + \nabla \cdot (\rho\, \boldsymbol{\xi}) = 0, & \text{(2.1a)} \\ \dfrac{\partial (\rho \boldsymbol{\xi})}{\partial t} + \nabla \cdot (\rho \boldsymbol{\xi} \otimes \boldsymbol{\xi}) = \rho \boldsymbol{\mathcal{A}}[\rho, \boldsymbol{\xi}, u; \boldsymbol{x}], & \text{(2.1b)} \\ \dfrac{\partial (\rho u)}{\partial t} + \nabla \cdot (\rho u \boldsymbol{\xi}) = \rho \mathcal{B}[\rho, \boldsymbol{\xi}, u; \boldsymbol{x}], & \text{(2.1c)} \end{cases}$$

where the square brackets indicate that $\boldsymbol{\mathcal{A}}$ and $\mathcal{B}$ depend functionally on the density, velocity and activity fields, and locally on the spatial position $\boldsymbol{x}$.

Impermeability conditions, similar to those used in fluid dynamics, are applied to enforce restrictions on pedestrian movement at walls,

$$\boldsymbol{\xi} \cdot \boldsymbol{n} = 0, \qquad \boldsymbol{x} \in \partial\Omega - \partial\Omega_e, \tag{2.2}$$

where $\partial\Omega_e$ are the points of the boundary representing exits and $\boldsymbol{n}$ is the unit vector normal to the boundary.

To establish a closed system, it is necessary to provide expressions for the source terms $\boldsymbol{\mathcal{A}}$ and $\mathcal{B}$ in Eqs.(2.1b) and (2.1c), and this requires specifying the social behavior to be modeled. Subsection 2.1 provides general guidelines for modelling these source terms, while subsection 2.2 focuses on detailed expressions, particularly when the activity variable represents stress and contagion awareness.

It should be noted that Eqs. (2.1) and (2.2), as well as equations that will be presented in the following sections, are expressed in dimensionless form. As reference quantities for density, position, and velocity, we assumed the maximum pedestrian packing (i.e., 6 people per square meter), a characteristic length (i.e., 1 m), and the highest average speed that pedestrians can achieve in a low-density flow within a high-quality venue (i.e., 5 km/h), respectively. The use of dimensionless quantities is intended to ensure that model variables such as density and velocity vary between zero and one. However, there is no mathematical proof that these bounds are met when the model is solved numerically. Exceeding these bounds indicates a departure from physical relevance and invalidates the numerical results.

2.1. *Modelling the source terms*

While the specific expressions for the source terms depend on the social dynamics being modeled, a common assumption that applies consistently across different social dynamics is that pedestrians make decisions about their walking behavior in a sequential fashion. First, they choose their walking direction, and then adjust their speed and modify their activity based on the local flow conditions and those in the chosen direction of movement. The source terms can thus be modeled as

$$\boldsymbol{\mathcal{A}}[\rho, \boldsymbol{\xi}, u; \boldsymbol{x}, t] = \varphi[\rho, u; \boldsymbol{\omega}, \boldsymbol{x}]\, \boldsymbol{\omega}, \tag{2.3a}$$

$$\mathcal{B}[\rho, \boldsymbol{\xi}, u; \boldsymbol{x}, t] = \psi[u; \boldsymbol{\omega}], \tag{2.3b}$$

where the two functional expressions φ and ψ depend on the particular social dynamics under consideration, and $\boldsymbol{\omega} = \boldsymbol{\omega}[\rho, \boldsymbol{\xi}, u; \boldsymbol{x}]$ is the walking direction.

Furthermore, in our modeling approach, which builds on the foundation laid by previous kinetic theory models [5], we assume that the pedestrians' choice of walking direction is made based on three guiding stimuli, represented as unit vector fields $\boldsymbol{\nu}_T$, $\boldsymbol{\nu}_S$, and $\boldsymbol{\nu}_V$. These fields correspond to the desire to reach a defined destination, $\boldsymbol{\nu}_T$, the attraction of the mean flow, $\boldsymbol{\nu}_S$, and the attempt to avoid crowded areas, $\boldsymbol{\nu}_V$.

Specifically, the *target direction*, denoted as $\boldsymbol{\nu}_T$, is a spatially dependent and time-invariant unit vector field. It indicates the direction at any spatial location that efficiently guides pedestrians to their destinations, where 'efficiently' is subject to different definitions. While other approaches could have been used, in this paper this field was determined by solving a Poisson equation for a potential field ϕ,

assuming that ϕ has a value of zero at the exit points and unity elsewhere, i.e.,

$$\begin{cases} \nabla\phi = 0, & \boldsymbol{x} \in \Omega, \\ \phi = 1, & \boldsymbol{x} \in \partial\Omega - \partial\Omega_e, \\ \phi = 0, & \boldsymbol{x} \in \partial\Omega_e, \end{cases} \tag{2.4}$$

and then normalizing the solution to unity. Note that this produces a vector field $\boldsymbol{\nu}_T$ analogous to the streamlines of an incompressible fluid flowing out of the domain. The *vacuum direction*, $\boldsymbol{\nu}_V$, and *stream direction*, $\boldsymbol{\nu}_S$, are unit vector fields that vary in space and time through their dependence on the density and velocity fields, respectively. The former indicates the direction of the lowest density at any point in space while the latter is the direction of movement when pedestrians are herding. They are defined as

$$\boldsymbol{\nu}_V = -\frac{\nabla\rho}{||\nabla\rho||}, \qquad \boldsymbol{\nu}_S = \frac{\boldsymbol{\xi}}{||\boldsymbol{\xi}||}. \tag{2.5}$$

Based on the discussion above, the walking direction is expressed as

$$\boldsymbol{\omega}[\rho, \boldsymbol{\xi}, u; \boldsymbol{x}] = \boldsymbol{\omega}(\boldsymbol{\nu}_T, \boldsymbol{\nu}_S, \boldsymbol{\nu}_V; \rho, u), \tag{2.6}$$

where we assume that, in addition to the three unit vectors, pedestrian choices are also influenced by local density conditions and activity levels

2.2. *Modelling stress and contagion awareness*

The definition of the pedestrians' walking direction $\boldsymbol{\omega}$ plays a critical role in the modeling of the source terms, as shown in Eqs. (2.3). Initially, pedestrians choose a tentative walking direction, $\boldsymbol{\omega}^*$, based on local density conditions, where higher local densities encourage walking toward less crowded areas, while lower densities steer pedestrians toward their intended destination. However, their choice evolves when their activity factor becomes relevant. Specifically, when the activity represents a state of stress, higher levels of stress result in a more pronounced tendency toward the mean flow (i.e., herding behavior). Conversely, when the activity represents contagion awareness, heightened awareness increases the tendency to deviate from the mean flow.

This modelling approach translates into the following mathematical structure.

(1) Selection of the walking direction: If the density is high, pedestrians will move away from the more crowded areas, in the direction of $\boldsymbol{\nu}_V$, whereas, if the density is low, pedestrians will move toward the target identified by $\boldsymbol{\nu}_T$. Therefore, the tentative walking direction is

$$\boldsymbol{\omega}^* = \frac{\rho\,\boldsymbol{\nu}_V + (1-\rho)\boldsymbol{\nu}_T}{||\rho\,\boldsymbol{\nu}_V + (1-\rho)\boldsymbol{\nu}_T||}. \tag{2.7}$$

However, when pedestrians are under stress, they will tend to deviate from $\boldsymbol{\omega}$ and follow the mean flow as indicated by $\boldsymbol{\nu}_S$, while the opposite happens when pedestrians are aware of potential contagion. Accordingly, the final walking directions $\boldsymbol{\omega}$ when pedestrains are under stress (denoted by $\boldsymbol{\omega}_s$) and under contagion awareness (denoted by $\boldsymbol{\omega}_c$) are as follows

- Stress:

$$\boldsymbol{\omega}_s = \frac{u\,\boldsymbol{\nu}_S + (1-u)\boldsymbol{\omega}^*}{||u\,\boldsymbol{\nu}_S + (1-u)\boldsymbol{\omega}^*||}. \tag{2.8a}$$

- Contagion awareness:

$$\boldsymbol{\omega}_c = \frac{(1-u)\,\boldsymbol{\nu}_S + u\boldsymbol{\omega}^*}{||(1-u)\,\boldsymbol{\nu}_S + u\boldsymbol{\omega}^*||}. \tag{2.8b}$$

After choosing their walking direction, pedestrians adjust their speed and their activity changes based on the local density and activity, as well as the density gradients ahead. Specifically, under stress (contagion awareness), pedestrians decelerate when facing crowded areas ahead, with the amount of deceleration influenced by their stress level and local density. Higher stress leads to less (more) deceleration, and higher local density leads to more deceleration. Conversely, less crowded areas ahead cause pedestrians to accelerate, with higher stress increasing (decreasing) this acceleration tendency and higher local density dampening it.

Regarding the activity variable, whether it represents stress or contagion awareness, pedestrians are assumed to mimic the activity levels they perceive, increasing their own activity when the level in the walking direction is higher and decreasing it when the level is lower.

This modeling approach translates into the following mathematical structure.

(2) Selection of the walking speed: Pedestrians tend to adjust their walking speed based on density and activity fields,

$$\varphi[\rho, u; \boldsymbol{\omega}, \boldsymbol{x}] = \alpha(\boldsymbol{x})\, a[\rho, u]\, \boldsymbol{\omega}, \tag{2.9}$$

where α is a scalar field denoting the quality of the environment in which pedestrians walk, and the functional a takes different expressions depending on whether it refers to pedestrians under stress (denoted by a_s) and under contagion awareness (denoted by a_c), i.e.,

- Stress:

$$a_s[\rho, u] = w(\partial_{\boldsymbol{\omega}}\rho)\ \left[\rho(1-u)H(\partial_{\boldsymbol{\omega}}\rho) + (1-\rho)uH(-\partial_{\boldsymbol{\omega}}\rho)\right], \tag{2.10a}$$

- Contagion awareness:

$$a_c[\rho, u] = w(\partial_{\boldsymbol{\omega}}\rho)\ \left[\rho u H(\partial_{\boldsymbol{\omega}}\rho) + (1-\rho)(1-u)H(-\partial_{\boldsymbol{\omega}}\rho)\right]. \tag{2.10b}$$

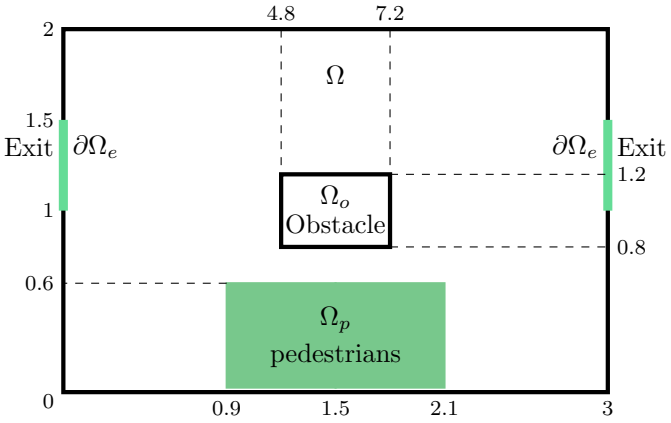

Figure 1. Geometry of the walking venue, where Ω represents the entire domain, Ω_o corresponds to the region occupied by obstacles, $\partial\Omega_e$ denotes the exits, and Ω_p indicates the area where pedestrians are initially located.

In Eqs. (2.10), $H(\cdot)$ is the Heaviside function that takes zero/one for negative/positive arguments, and $w(\cdot)$ is a weighting function that depends on the derivative of the density in the walking direction, i.e.,

$$w(\partial_{\boldsymbol{\omega}}\rho) = -\frac{\partial_{\boldsymbol{\omega}}\rho}{\sqrt{1+(\partial_{\boldsymbol{\omega}}\rho)^2}}, \tag{2.11}$$

so that $w \to \mp 1$ when $\partial_{\boldsymbol{\omega}}\rho \to \mp\infty$.

(3) Update of the activity: Pedestrians modulate their own activity levels based on the activity levels they perceive around them,

$$\psi[u;\boldsymbol{\omega}] = \beta\,(u_{\boldsymbol{\omega}} - u)\,, \tag{2.12}$$

where β is a constant and $u_{\boldsymbol{\omega}}$ is the perceived activity in the walking direction defined as

$$u_{\boldsymbol{\omega}} = u + \frac{\partial_{\boldsymbol{\omega}}u}{\sqrt{1+(\partial_{\boldsymbol{\omega}}u)^2}}\left[(1-u)\,H(\partial_{\boldsymbol{\omega}}u) + u\,H(-\partial_{\boldsymbol{\omega}}u)\right], \tag{2.13}$$

Note that $u_{\boldsymbol{\omega}} \to 0$ and 1 when $\partial_{\boldsymbol{\omega}}u \to \mp\infty$.

3. Numerical results

This section is devoted to the numerical resolution of the model presented in Section 2. First, the numerical method used and the simulation setup are presented. Then, two case studies are discussed to assess the model's ability to capture the complex crowd behavior resulting from the interplay between pedestrian psychology and collective dynamics.

3.1. *Numerical scheme and simulation setup*

The macroscopic model is solved numerically using the Finite Volume Method (FVM) [15,11] to ensure that the balance properties inherent in the continuum formulation of the model are preserved within the discrete equations. The set of macroscopic equations, Eqs. (2.1), can be rewritten as

$$\frac{\partial \boldsymbol{U}}{\partial t} + \frac{\partial \boldsymbol{F}}{\partial x} + \frac{\partial \boldsymbol{G}}{\partial y} = \boldsymbol{S}, \tag{3.1}$$

where

$$\boldsymbol{U} = \begin{bmatrix} \rho \\ \rho\xi_x \\ \rho\xi_y \\ \rho u \end{bmatrix}, \quad \boldsymbol{F} = \begin{bmatrix} \rho\xi_x \\ \rho\xi_x^2 \\ \rho\xi_x\xi_y \\ \rho\xi_x u \end{bmatrix}, \quad \boldsymbol{G} = \begin{bmatrix} \rho\xi_y \\ \rho\xi_x\xi_y \\ \rho\xi_y^2 \\ \rho\xi_y u \end{bmatrix}, \quad \boldsymbol{S} = \begin{bmatrix} 0 \\ \rho\phi\omega_x \\ \rho\phi\omega_y \\ \rho\psi \end{bmatrix}. \tag{3.2}$$

We use the Lax-Friedrichs scheme [9], which discretizes the system of equations forward in time and centered in space, yielding

$$U_{i,j}^{n+1} = U_{i,j}^n - \Delta t_n \left[\frac{F_{i+\frac{1}{2},j}^n - F_{i-\frac{1}{2},j}^n}{\Delta x} + \frac{G_{i,j+\frac{1}{2}}^n - G_{i,j-\frac{1}{2}}^n}{\Delta y} \right] + \Delta t_n S_{i,j}^n, \tag{3.3a}$$

where

$$F_{i\pm\frac{1}{2},j}^n = \frac{1}{2}[F(U_{i,j}^n) + F(U_{i\pm1,j}^n) \pm \alpha_x^n (U_{i,j}^n - U_{i\pm1,j}^n)], \tag{3.3b}$$

$$G_{i,j\pm\frac{1}{2}}^n = \frac{1}{2}[G(U_{i,j}^n) + G(U_{i,j\pm1}^n) \pm \alpha_y^n (U_{i,j}^n - U_{i,j\pm1}^n)], \tag{3.3c}$$

being

$$\alpha_x^n = \max_{i,j}(\xi_x)_{i,j}^n, \quad \alpha_y^n = \max_{i,j}(\xi_y)_{i,j}^n. \tag{3.3d}$$

In Eq. (3.3a), the time step $\Delta t_n = \min\{\Delta x/\alpha_x^n, \Delta y/\alpha_y^n\}$ is adjusted for each n to satisfy the CFL condition.

In all simulations discussed below, we use $\alpha = 1$ in Eq. (2.9) over the entire domain, $\beta = 1$ in Eq. (2.12), and we consider a rectangular computational domain Ω, as shown in Fig. 1. The domain Ω is discretized using a uniform mesh with a grid size of $\Delta x = \Delta y = 0.02$. There are two exits labeled $\partial\Omega_e \subset \partial\Omega$ on the boundary - one on the left and one on the right - for outflow purposes only. The remaining part of the domain boundary, $\partial\Omega - \partial\Omega_e$, is considered an impenetrable wall, like the obstacle inside the domain, bounded by a rectangular region labeled Ω_o. Specifically, the impenetrability condition is

$$\boldsymbol{\xi} \cdot \boldsymbol{n} = 0, \qquad \boldsymbol{x} \in (\partial\Omega - \partial\Omega_e) \cup \partial\Omega_o, \tag{3.4}$$

where $\boldsymbol{n}$ is the unit vector normal to the wall.

In conjunction with the previously defined boundary conditions, Eqs.(3.3) are supplemented with initial conditions that specify values of the density ρ_0, velocity ξ_o, and activity u_0 fields over the region $\Omega_p \subset \Omega$ initially occupied by pedestrians.

3.2. *Case studies*

In this subsection, we present two representative case studies for which the model is solved numerically. In addition to contour plots of the density and activity fields, two gross quantities are computed to gain further insight into the pedestrian dynamics during exit. First, the normalized pedestrian density, $\mathcal{N}$, namely the fraction of pedestrians in the domain divided by the initial number of pedestrians, which allows us to determine the exit time. Second, the mean activity, $\mathcal{U}$, which is a proxy for social dynamics. Mathematically, these quantities are defined as follows:

$$\mathcal{N} = \frac{\int_\Omega \rho d\boldsymbol{x}}{\int_\Omega \rho_0 d\boldsymbol{x}}, \qquad \mathcal{U} = \frac{\int_\Omega \rho u d\boldsymbol{x}}{\int_\Omega \rho d\boldsymbol{x}}. \tag{3.5}$$

Case study I: Evacuation under stress vs. contagion awareness

In this case study, we compare crowd evacuation dynamics under the two proposed social behaviors, namely stress and contagion awareness. Specifically, we ran two separate and independent simulations with identical boundary and initial conditions. The initial crowd was at rest, uniformly distributed over the domain Ω_p with a density of $\rho_0 = 0.5$ and an activity of $u_0 = 0.8$, representing the stress in one simulation and contagion awareness in the other. The symmetry of the initial and boundary conditions ensures that symmetry is maintained in both halves of the domain throughout the evacuation. Therefore, the two social dynamics are contrasted with side-by-side snapshots of the density and activity fields in Figs. 2 and 3, respectively, where pedestrians move under stress on the left and under contagion awareness on the right. This comparative approach provides an insightful understanding of how different social behaviors affect evacuation time, flow rates, and congestion.

As can be seen in Fig. 2(a)-(b) and Fig. 4(a), the crowd under stress initially accelerates faster and starts evacuating earlier than under contagion awareness. This is consistent with the acceleration models given by Eqs. (2.10), which predict a higher acceleration of pedestrians under stress when close to vacuum regions. The activity contour plots in Figures 3(a)-(f) show that stress and contagion awareness spread through the crowd at different rates. The activity contours for stress were nearly uniform, indicating rapid spread throughout the domain, whereas the activity contours for contagion awareness have localized areas of high and low values. Furthermore, as evacuation progresses, the mean activity decreases in both cases, but with a steeper negative slope for contagion awareness, as shown in Fig. 4(b).

By contrasting the two social dynamics, we can see that stress spreads faster than contagion awareness and is also a more deeply rooted social trait. This is because pedestrians with contagion awareness do not exhibit the herding behavior typical of evacuations under stress. Herding behavior leads to the formation of high-density regions near walls, as shown in Fig. 2(c)-(d), where pedestrian stress levels increase and become more persistent.

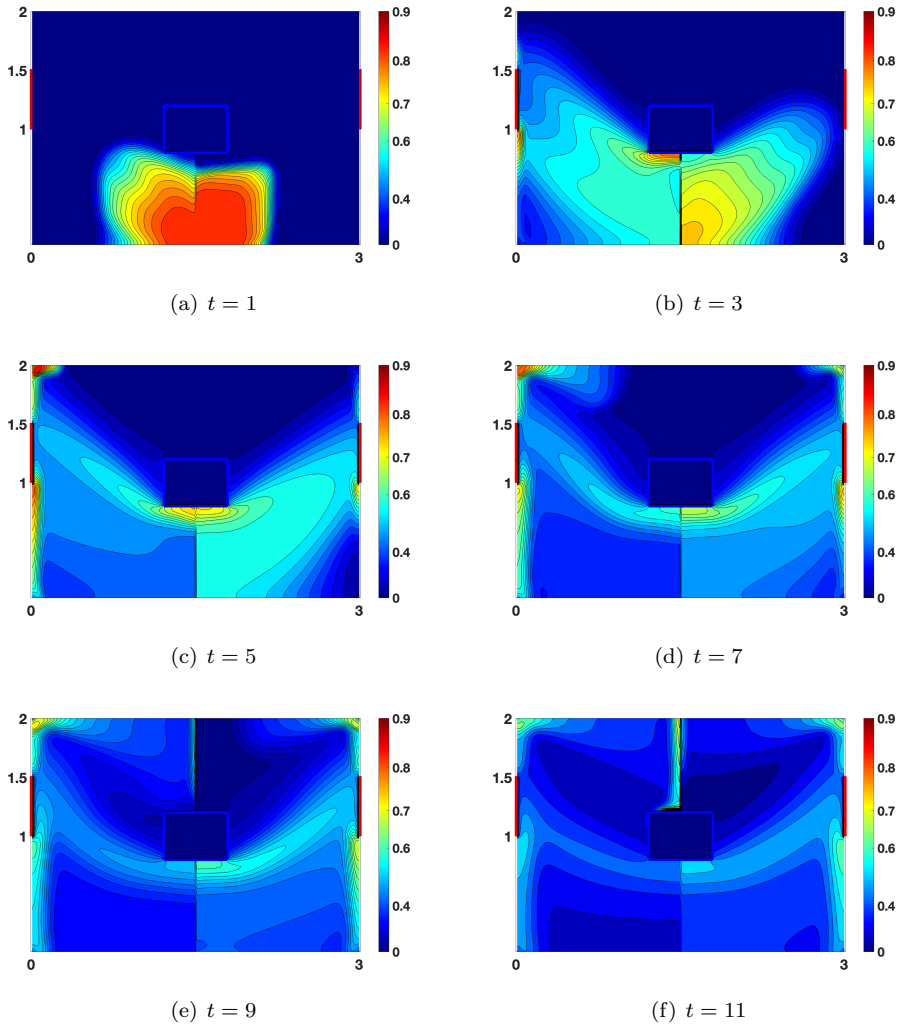

(a) $t = 1$ (b) $t = 3$

(c) $t = 5$ (d) $t = 7$

(e) $t = 9$ (f) $t = 11$

Figure 2. Case study I: Snapshots of the density field contour plots. Left side: Evacuation under stress; Right side: Evacuation under contagion awareness.

Case study II: Evacuation under stress during an incident

In this case study, the activity variable is used to represent the pedestrians' stress level, and the goal is to demonstrate how our model can capture stress changes during an emergency caused by a restricted exit. Specifically, we simulate an incident where an exit suddenly closes at time $t_c = 6$, forcing pedestrians to reroute to the remaining open exit. Initially, the crowd is divided into two groups at rest with identical activity, $u_0 = 0.5$, but different densities of 0.7 (right group) and 0.3 (left group). These different density values are used to assess their effect on the dynamics

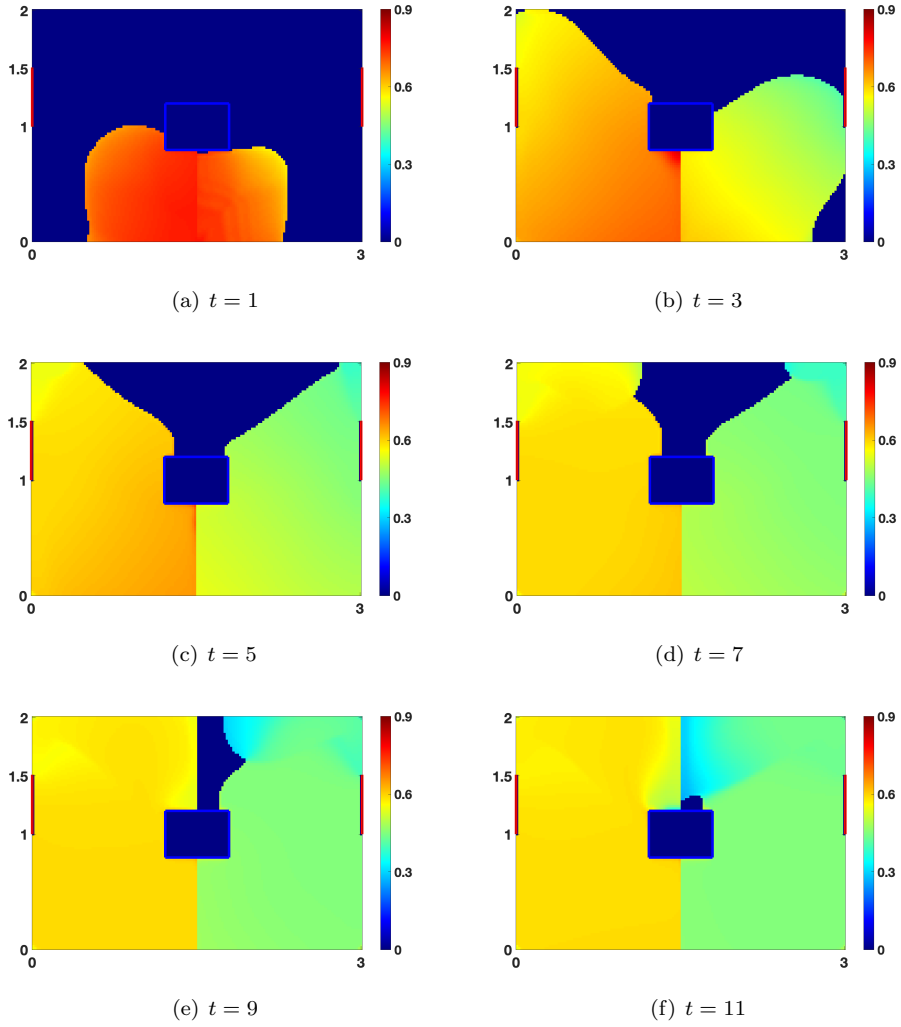

(a) $t = 1$ (b) $t = 3$

(c) $t = 5$ (d) $t = 7$

(e) $t = 9$ (f) $t = 11$

Figure 3. Case study I: Snapshots of the activity field contour plots. Left side: Evacuation under stress; Right side: Evacuation under contagion awareness.

of the crowd and the propagation of stress.

Despite the asymmetric initial conditions, the early pedestrian flow appears symmetric overall. However, there are pedestrians that move from the right side of the domain to the left as shown in Fig. 7(a). This migration is expected as pedestrians initially try to avoid the more crowded area on the right. Fig. 7(b) shows that the mean activity of both groups decreases similarly early on as pedestrians can find less crowded areas to move to, thus reducing their stress levels.

When the right exit abruptly closes at time t_c, the target direction field is imme-

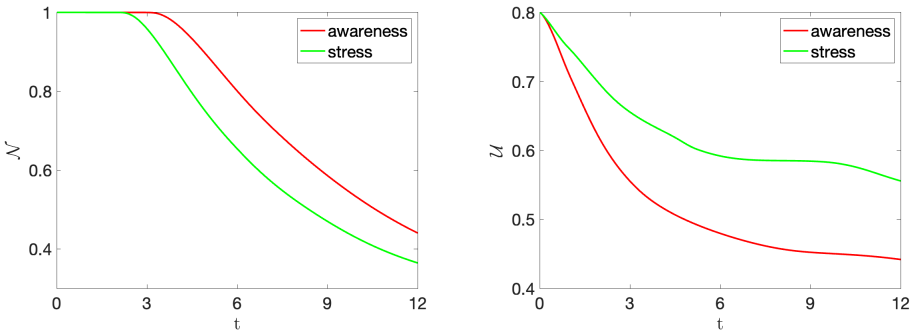

(a) Normalized pedestrian density (b) Mean activity

Figure 4. Case study I: Mean quantities during evacuation.

diately recalculated based on the changed geometry, so that pedestrians only move towards the remaining open left exit. In fact, the density contours in Fig. 5(c)-(d) show that pedestrians on the right are gradually redirected to the left, which is further evidenced by the slight negative slope in Fig. 7(a) for $6 \lesssim t \lesssim 13$. Interestingly, Fig. 7(b) shows a sharp increase in mean activity after t_c, confirming that the exit closure event causes an increase in overall pedestrian stress levels.

In addition, large activity values appear on the right side starting at t_c, as shown in Fig. 6(c), indicating that the sudden loss of the exit creates tension and discomfort for pedestrians due to diversion and crowding effects. This demonstrates the ability of the model to accurately capture these real world phenomena.

4. Conclusions

In this paper, we have proposed a novel macroscopic modeling framework to describe the dynamics of social crowds. There are two main innovations. First, the introduction of an activity variable that captures the evolving psychological states of pedestrians, such as stress or contagion awareness. This allows modeling the complex interplay between pedestrian psychology and crowd dynamics, which has not been done before at the macroscopic level. Second, the "mechanical" and "social" behaviors of the crowd are coupled by a second-order crowd model. This allows for a more accurate description of dynamic situations involving pedestrian acceleration or deceleration.

We demonstrated the capabilities of the model by applying it to pedestrian egress scenarios and examining the role of activity in shaping crowd flow patterns. The case studies showed that dynamic changes in activity, representing stress or awareness, can significantly alter crowd behavior. This highlights the need to move beyond models that make static assumptions about pedestrian psychology.

The proposed approach opens up exciting research directions for developing more

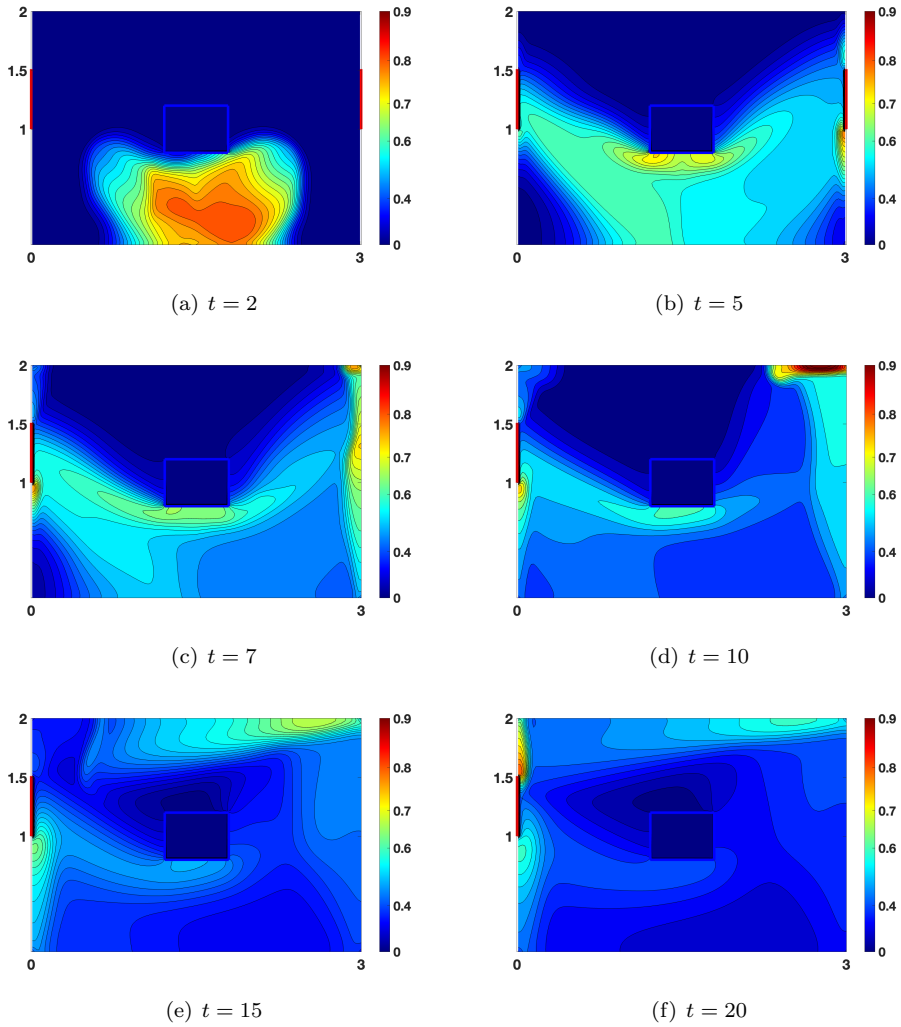

(a) $t = 2$ (b) $t = 5$

(c) $t = 7$ (d) $t = 10$

(e) $t = 15$ (f) $t = 20$

Figure 5. Case study II: Snapshots of the density field contour plots (the right door is closed at $t_c = 6$).

realistic macroscopic models of social crowds, with important practical implications for crowd management and safety. Future work can build on the foundation established in this paper to include additional psychological factors beyond stress and awareness. For example, emotional states such as anger or fear that cause demonstrators to shift from peaceful to riotous behavior, or crowd leadership dynamics, social ties, and communication networks that influence cooperative behavior in response to a natural disaster or terrorist attack. Incorporating these factors into models can greatly expand the breadth of applications that can be studied.

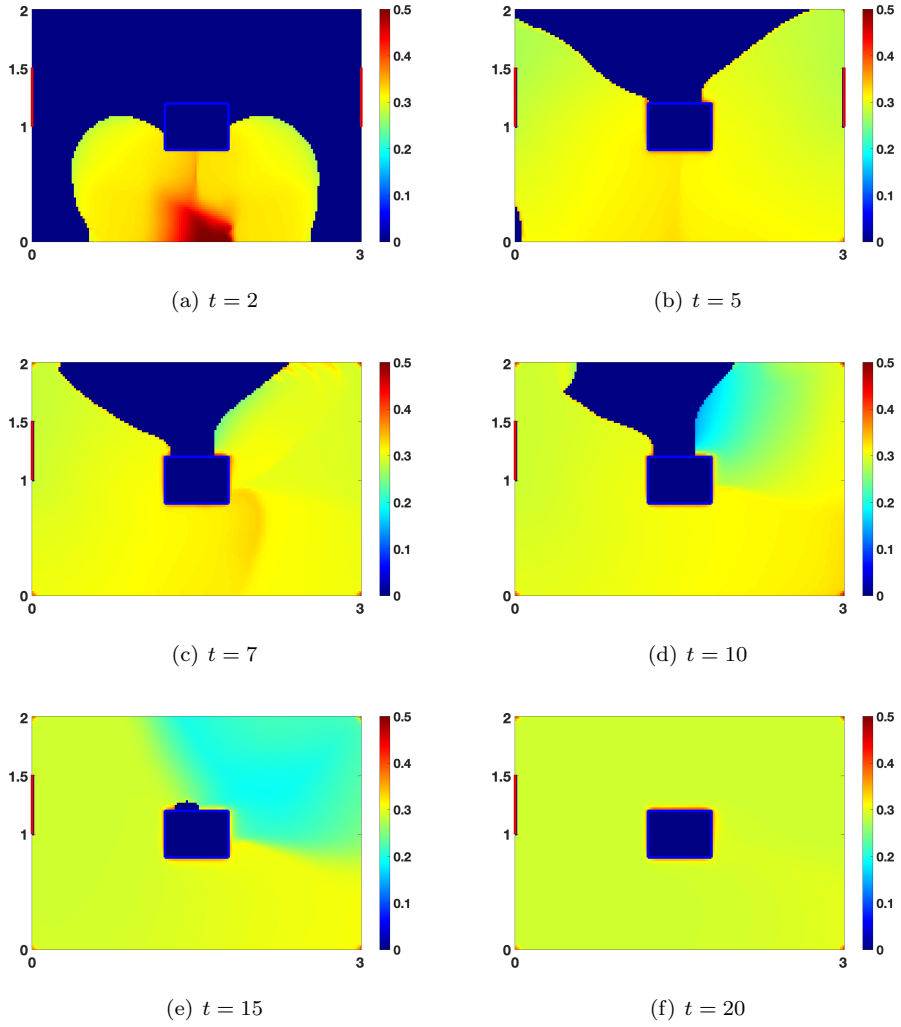

(a) $t = 2$ (b) $t = 5$

(c) $t = 7$ (d) $t = 10$

(e) $t = 15$ (f) $t = 20$

Figure 6. Case II: Snapshots of the activity field contour plots (the right door is closed at $t_c = 6$).

Acknowledgements

DK acknowledges the support of Agencia Nacional de Promoción de la Investigación, el Desarrollo Tecnológico y la Innovación through Project PICT 2021-0188.

Bibliography

1. J.P. Agnelli, B. Buffa, D.A. Knopoff and G. Torres, A spatial kinetic model of crowd evacuation dynamics with infectious disease contagion, *Bulletin of Mathematical Biology*, **85(4)**, 23, (2023).
2. J. Barreiro-Gomez and N. Masmoudi, Differential games for crowd dynamics and

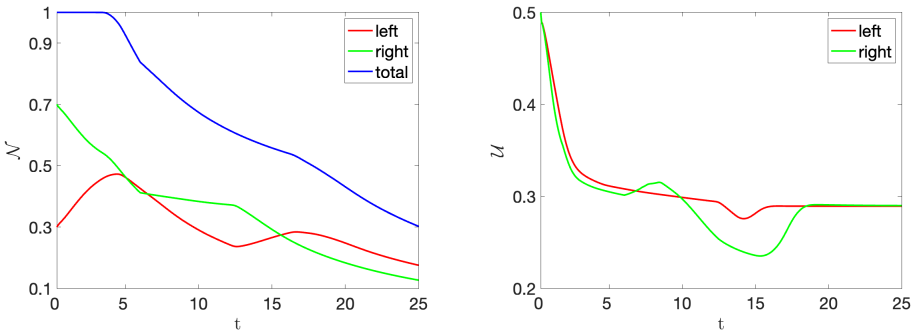

(a) Normalized pedestrian density (b) Mean activity

Figure 7. Case study II: Mean quantities during evacuation (the right door is closed at $t_c = 6$).

applications, *Mathematical Models and Methods in Appllied Sciences*, 1-40, (2023).

3. N. Bellomo, R. Bingham, M. A. J. Chaplain, G. Dosi, G. Forni, D. A. Knopoff, J. Lowengrub, R. Twarock and M. E. Virgillito, A multi-scale model of virus pandemic: Heterogeneous interactive entities in a globally connected world, *Mathematical Models and Methods in Applied Sciences*, **30(8)**, 1591–1651, (2020).
4. N. Bellomo, D. Burini, G. Dosi, L. Gibelli, D. A. Knopoff, N. Outada, P. Terna and M.E. Virgillito, What is life? A perspective of the mathematical kinetic theory of active particles, *Mathematical Models and Methods in Applied Sciences*, **31(9)**, 1821–1866, (2021).
5. N.Bellomo, L. Gibelli and N. Outada, On the interplay between behavioral dynamics and social interactions in human crowds, *Kinetic and Related Models*, **12**, 397–409, (2019).
6. N. Bellomo, L. Gibelli, A. Quaini and A. Reali, Towards a mathematical theory of behavioral human crowds, *Mathematical Models and Methods in Applied Sciences*, **32(2)**, 321–358, (2022).
7. N. Bellomo, J. Liao, A. Quaini, L. Russo and C. Siettos, Human behavioral crowds: Review, critical analysis, and research perspectives, *Mathematical Models and Methods in Applied Sciences*, **33(8)**, 1611-1659, (2023).
8. A.L. Bertozzi, J. Rosado, M.B. Short and L. Wang, Contagion shocks in one dimension, *Journal Statistical Physics*, **158(3)**, 647–664, (2015).
9. F. Bouchut, **Nonlinear stability of finite Volume Methods for hyperbolic conservation laws: And Well-Balanced schemes for sources**, Springer Science & Business Media, (2021).
10. D. Burini, S. De Lillo and L. Gibelli, Stochastic differential "nonlinear" games modeling collective learning dynamics, *Physics of Life Reviews*, **16**, 123–139, (2016).
11. J.A. Carrillo, S. Martin and M.T. Wolfram, An improved version of the Hughes model for pedestrian flow, *Mathematical Models and Methods in Applied Sciences*, **26(4)**, 671–697, (2016).
12. R.M. Colombo and M.D. Rosini, Pedestrian flows and non-classical shocks, *Mathematical Methods in the Applied Sciences*, **28(13)**, 1553–1567, (2005).
13. E. Cristiani, B. Piccoli and A. Tosin, **Multiscale Modeling of Pedestrian Dynamics**, Springer, 2014.
14. H. Ennaji, N. Igbida and G. Jradi, Prediction-Correction Pedestrian Flow by Means

of Minimum Flow Problem, *Mathematical Methods in the Applied Sciences*, to appear (2023).
15. P. Goatin and M. Mimault, Mixed system modeling two-directional pedestrian flows, *Mathematical Biosciences & Engineering*, **12(2)**, 375–392, (2015).
16. D. Helbing, Traffic and related self-driven many-particle systems, *Review Modern Physics* **73**, 1067–1141, (2001).
17. D. Helbing and A. Johansson, Pedestrian, crowd and evacuation dynamics, *Encyclopedia of Complexity and Systems Science*, 6476–6495, (2010).
18. D. Helbing, A. Johansson and H.-Z. Al-Abideen, Dynamics of crowd disasters: An empirical study, *Physics Review E*, **75**, 046109, (2007).
19. D. Kim, K. O'Connell, W. Ott and A. Quaini, A kinetic theory approach for 2D crowd dynamics with emotional contagion, *Mathematical Models and Methods in Applied Sciences*, **31(6)**, 1137–1162, (2021).
20. D. Kim and A. Quaini, Coupling kinetic theory approaches for pedestrian dynamics and disease contagion in a confined environment, *Mathematical Models and Methods in Applied Sciences*, **30(10)**, 1893–1915, (2020).
21. H. Liang, J. Du and S.C. Wong, A continuum model for pedestrian flow with explicit consideration of crowd force and panic effects, *Transportation Research Part B: Methodological*, **149**, 100-117, (2021).
22. J. Liao, Y. Ren and W. Yan, Kinetic modeling of a leader–follower system in crowd evacuation with collective learning *Mathematical Models and Methods in Applied Sciences*, **33(5)**, 1099–1117, (2023).
23. L. Pareschi and G. Toscani, **Interacting Multiagent Systems: Kinetic Equations and Monte Carlo Methods** Oxford University Press, Oxford, (2013).
24. L. Wang, M.B. Short and A.L. Bertozzi, Efficient numerical methods for multiscale crowd dynamics with emotional contagion, *Mathematical Models and Methods in Applied Sciences*, **27(1)**, 205–230, (2017).